



Structural abnormality of the hippocampus associated with depressive symptoms in heart failure rats



Hideaki Suzuki ^{a,*}, Akira Sumiyoshi ^b, Yasuharu Matsumoto ^a, Ben A. Duffy ^c, Takeo Yoshikawa ^d, Mark F. Lythgoe ^c, Kazuhiko Yanai ^d, Yasuyuki Taki ^e, Ryuta Kawashima ^b, Hiroaki Shimokawa ^a

^a Department of Cardiovascular Medicine, Tohoku University Graduate School of Medicine, Sendai, Japan

^b Department of Functional Brain Imaging, Institute of Development, Aging and Cancer, Tohoku University, Sendai, Japan

^c Centre for Advanced Biomedical Imaging (CABI), Department of Medicine and Institute of Child Health, University College London (UCL), UK

^d Department of Pharmacology, Tohoku University Graduate School of Medicine, Sendai, Japan

^e Department of Nuclear Medicine and Radiology, Institute of Development, Aging and Cancer, Tohoku University, Sendai, Japan

ARTICLE INFO

Article history:

Accepted 14 October 2014

Available online 22 October 2014

Keywords:

Voxel based morphometry

Histology

Depression

Hippocampus

Heart failure

ABSTRACT

Heart failure (HF) is characterized by a blood supply which is insufficient to meet the body's demand. HF can potentially affect the brain and is associated with a high prevalence of depression. However, the mechanisms by which the two are related remain largely unclear. Structural abnormalities of the ventral hippocampus have been observed in depression but have never been reported in HF. In this study, we thus investigated structural brain abnormality in HF using voxel-based morphometry (VBM) and histological analysis in a rat model of HF. T2-weighted images were obtained in rats with HF ($n = 20$) and sham rats ($n = 17$) and VBM was used to produce gray matter concentration (GMC) maps. Twenty-four hour locomotor activity was used as a sign of depressive behavior. Brains of HF and sham rats ($n = 8$, each) were fixed and histologically analyzed for the measurement of neurogenesis, the number of astrocytes and neurite outgrowth in the ventral hippocampus. VBM demonstrated significant GMC decrease in the hippocampus, which was restricted to the ventral segment. Similarly, neurogenesis and neurite outgrowth were significantly decreased and the number of astrocytes was significantly increased in HF rats as compared with sham rats in the ventral hippocampus. GMC values in the ventral hippocampus were significantly and negatively correlated with 24 hour locomotor activity in HF rats. In conclusion, the present study has demonstrated for the first time that the structural abnormality of the ventral hippocampus is associated with depressive symptoms in HF rats.

© 2014 Elsevier Inc. All rights reserved.

Introduction

Heart failure (HF) is characterized by insufficient blood supply for the body demand due to cardiac dysfunction and often occurs as a result of myocardial ischemia. Low cardiac output and chronic stress in HF can potentially affect the brain. Prevalence of depression is increased among HF patients (Rutledge et al., 2006), which suggests that there may also be coexisting structural brain abnormalities. Depression complicated with HF is associated with increased risk of mortality and rehospitalization in patients with HF (Jiang et al., 2001; Rutledge et al., 2006) and thus should be investigated to improve outcomes. However, the mechanism of depression in HF remains largely unclear.

The hippocampus is an important brain center, which is involved in emotion and memory, and can be subdivided into the ventral and dorsal segments. Lesioning the ventral and dorsal hippocampi in rodents can

lead to aberrant expression of anxiety and memory deficits, respectively (Kjelstrup et al., 2002; Broadbent et al., 2004; Fanselow and Dong, 2010). Behaviorally depressed cynomolgus macaques showed reduced volume of the anterior hippocampus (Willard et al., 2009), which is analogous to the ventral hippocampus in rodents. The ventral hippocampus is more vulnerable to decreased neurogenesis than the dorsal hippocampus in rodent models of depression-like behavior (Tanti and Belzung, 2013). To the best of our knowledge, however, there is no definite evidence that structural abnormalities of the ventral hippocampus have been previously observed in HF.

Voxel-based morphometry (VBM), an unbiased technique based on magnetic resonance imaging (MRI), has been used to assess regional differences in the concentration or volume of a particular tissue such as brain gray matter (Ashburner and Friston, 2000, 2001; Quallo et al., 2009; Sawiak et al., 2009; Yang et al., 2011; Biedermann et al., 2012; Suzuki et al., 2013b). There have already been three VBM studies recruiting HF patients (Woo et al., 2003; Menteer et al., 2010; Almeida et al., 2012), which did not consistently reveal structural abnormalities of the hippocampus. Probably this is because patients with HF usually have many confounding factors affecting gray matter such as

* Corresponding author at: Department of Cardiovascular Medicine, Tohoku University Graduate School of Medicine, 1-1, Seiryō-machi, Aoba-ku, Sendai 980-8574, Japan. Fax: +81 22 717 7156.

E-mail address: hd.suzuki.1870031@cardio.med.tohoku.ac.jp (H. Suzuki).

hypertension, diabetes, dyslipidemia, smoking and administration of antihypertensive drugs (Ward et al., 2010; Zhang et al., 2011; Glodzik et al., 2012; Moran et al., 2013). Therefore, structural brain abnormalities in HF should be assessed using experimental animals that have uniform environmental and genetic backgrounds. We previously reported an in-vivo rat T2 MRI template that includes three different classes of tissue probability maps (Valdés-Hernández et al., 2011). VBM using our rat template could successfully detect structural abnormalities of the hippocampus in a rat model of cardiopulmonary resuscitation (Suzuki et al., 2013b).

In the present study, we assessed structural brain abnormality in HF using VBM and histological analysis in a rat model of HF. We examined changes in neurogenesis, the number of astrocytes and neurite outgrowth in the ventral and dorsal hippocampi histologically. Twenty-four hour locomotor activity, an index of depressive symptoms in rodents (Fukumauchi et al., 1996; Kabuki et al., 2009), was also measured in both HF and sham rats before MRI recordings. Increased locomotor activity in 24 hour spontaneous measurement is observed in rodent models of depression or chronic stress (Fukumauchi et al., 1996; Kabuki et al., 2009). The purpose of the present study was to investigate the following four hypotheses: (1) VBM detects gray matter changes in the ventral hippocampus in HF rats, (2) neurogenesis, the number of astrocytes and neurite outgrowth are changed in the ventral hippocampus in HF rats, (3) 24 hour locomotor activity is increased in HF rats, and (4) VBM-detected gray matter changes in HF rats are associated with depressed symptoms examined with 24 hour locomotor activity measurements.

Materials and methods

Animals

A total of 53 male Wistar rats (9 week-old; Charles River, Japan) were assigned to either HF group ($n = 28$) or sham group ($n = 25$). The HF and sham rats were used either for MRI recordings followed by behavioral tests (20 HF and 17 sham rats) or histological analysis (8 HF and 8 sham rats). All procedures and protocols were performed in accordance with the policies established by the Animal Care Committee at Tohoku University, Sendai, Japan (approval number: 2012-241).

The HF rats

The coronary ligation protocol was performed as previously described (Henderson et al., 2009). Briefly, rats were anesthetized with isoflurane, and were orally intubated for mechanical ventilation using a ventilator (Harvard Apparatus, Holliston, MA, USA). The following surgical preparations were performed in the prone position on a hotplate (AS ONE, Osaka, Japan) under 1.5% isoflurane. The chest was opened at the 4th intercostal space to expose the heart, the pericardium was incised and the left anterior descending coronary artery was ligated between the pulmonary outflow tract and the left atrium with a 6-0 silk suture. The lungs were re-inflated by momentarily occluding the outflow of the ventilator. The chest was closed with 3-0 silk sutures. Weight-matched rats were used as controls and underwent all surgical steps except for the coronary ligation (sham rat). The HF and sham rats were returned to their cages where they were housed for 16 weeks in a room on a 12-hr light–dark cycle until the time of the behavioral studies or histological analysis.

Behavioral tests

Sixteen weeks after the coronary ligation or the sham operation protocol, 24 hour locomotor activity measurement was performed as described in our previous study (Okuda et al., 2004). After adaptation for three days, 24 hour locomotor activity was measured using an infrared ray sensor system (SUPER-MEX, Muromachi-Kikai, Tokyo, Japan) that

consists of twelve small compartments divided with walls on a large shelf. The size of each compartment is 40 cm wide \times 50 cm long \times 35 cm high, and each compartment is equipped with a ceiling sensor that can detect heat energy radiated from the rats. The system monitors rat movement by measuring changes in heat energy in the covered field. Rats were placed individually in the compartments within steel wire cages.

Echocardiographic assessment

In vivo heart function and structure were assessed by echocardiography using a Vevo 2100 system (VisualSonics, Toronto, Ontario, Canada) designed specifically for small animal studies as previously described (Morgan et al., 2004). The echocardiographic assessment was performed before MRI recording or histological analysis and within 4 days of the 24 hour locomotor activity measurement. Rats were anesthetized with 2% isoflurane administered via a nose cone, were shaved from the chest and were placed in the supine position on a hotplate (AS ONE, Osaka, Japan). Two-dimensional (2D) and M-mode echocardiography images were obtained from the parasternal short-axis view to measure fractional shortening (FS), interventricular septal thickness (IVStd), left ventricular diastolic dimension (LVDD), left ventricular systolic dimension (LVDs) and posterior wall thickness in diastole (PWTd) (Fig. 1). FS was calculated as percentage in accordance with the following formula: $FS = (LVDD - LVDs) / LVDD \times 100(\%)$. All measurements were carried out offline using the Vevo 2100 system software and were averaged from three cardiac cycles.

MRI recording

MRI recording was performed as described in our previous studies (Sumiyoshi et al., 2012; Suzuki et al., 2013a,b). Briefly, rats were initially anesthetized with isoflurane, and polyethylene catheters were inserted into the femoral artery and vein to examine blood pressure and systemic drug delivery, respectively. The rats were orally intubated for artificial ventilation, were placed in the prone position on a custom-built MRI bed with a bite bar, and mechanically ventilated at a respiration rate of 60 ± 1 breaths/min using a ventilator (SAR-830/AP, CWE Inc., Ardmore, PA, USA). After the rats received a bolus injection of pancuronium (2 mg/kg), anesthesia was maintained at 1% isoflurane with continuous administration of pancuronium (2 mg/kg/h).

All MRI data were acquired using a 7.0 T Bruker PharmaScan system (Bruker Biospin, Ettlingen, Germany) with a 38-mm-diameter bird-cage coil. Prior to all MRI acquisitions, we first performed global magnetic field shimming inside the core and subsequently localized on the region of interest (ROI) using a point resolved spectroscopy protocol. The linewidth (full width at half maximum) at the end of the shimming procedure ranged from 10 to 16 Hz in the ROI (approximately 300 μ m). T2-weighted images (T2WIs) were obtained using a 2D-RARE sequence with the following parameters: TR = 4600 ms, TE_{eff} = 30 ms, RARE factor = 4, SBW = 100 kHz, flip angle = 90°, FOV = 32 \times 32 mm², matrix size = 256 \times 256, voxel size = 125 \times 125 μ m², number of slices = 54, slice thickness = 0.5 mm, slice gap = 0 mm, and number of repetitions = 10.

Measurement of cardiac infarct size

The measurement of infarct size protocol was performed as modified in the past study (Saeed et al., 2001). At the end of each MRI recordings, the heart was removed and was cross-sectioned from base to apex into four short-axis slices. The slices were weighed to measure heart weight and were immersed in distilled water that contained 1.0% triphenyltetrazolium chloride (TTC; Sigma Aldrich; Munich, Germany) for 20 min at 37 °C to identify infarcted tissue. Infarct size was calculated as mean value of infarct circumference divided by total

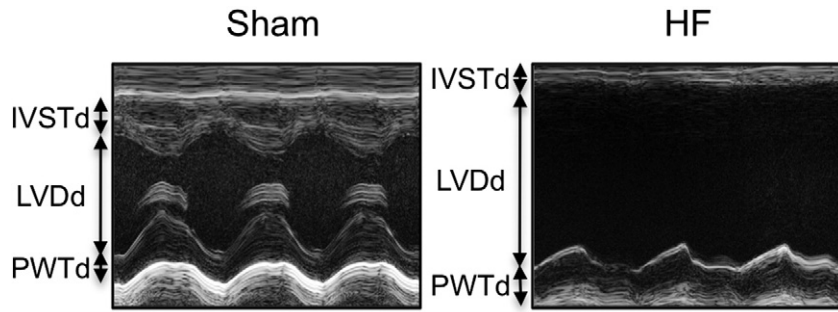


Fig. 1. Representative echocardiography of sham rat and HF rat. HF, heart failure; IVSTd, interventricular septal thickness in diastole; LVDd, left ventricular diastolic diameter; PWTd, posterior wall thickness in diastole.

circumference in each section times 100. Rats with small infarct size (<30%) were excluded from this study.

VBM analysis

T2WIs in HF ($n = 20$) and sham rats ($n = 17$) for the group comparison analysis and T2WIs in HF rats ($n = 20$) or sham rats ($n = 17$) for the voxel-based correlation analysis were analyzed using the statistical parametric mapping software (SPM8, Wellcome Department of Cognitive Neurology, London, UK) and custom-written software in MATLAB (Mathworks Inc., Natick, MA, USA). In the present study, VBM was performed as described in our previous studies (Taki et al., 2012; Suzuki et al., 2013b). First, the T2WIs were resized by a factor of 10 (Biedermann et al., 2012) and were realigned and resliced to adjust for head motion. The realigned anatomical images were then averaged to produce mean images. Second, after the mean images were aligned with the Wistar rat template brain (Valdés-Hernández et al., 2011), they were segmented into images of gray matter (GM), white matter (WM) and cerebrospinal fluid (CSF) by applying a unified segmentation approach (Ashburner and Friston, 2005) using the probabilistic maps of the Wistar rat brain (Valdés-Hernández et al., 2011). The obtained GM, WM and CSF images and T2WIs were rigid-body aligned (3 rotations and 3 translations) to the Wistar rat brain template (Valdés-Hernández et al., 2011) and were resampled to 1.25 mm (for the resized images) isotropic voxels. Third, the aligned GM, WM and CSF images were used to create a customized, more population-specific template using Diffeomorphic Anatomical Registration using Exponentiated Lie Algebra (DARTEL) template-creation tool (Ashburner, 2007). DARTEL has been shown to produce a more accurate registration than the standard VBM procedure (Klein et al., 2009) and is potentially suitable for performing VBM using probability maps from different rat strains. Fourth, each rat's gray matter image was warped using its corresponding smooth, reversible deformation parameters to transform it to the custom template space and then to the Wistar rat template space. Finally, the warped unmodulated or modulated gray matter images were smoothed with an isotropic Gaussian kernel to produce gray matter concentration (GMC) maps respectively by convolving an 8-mm (for the resized images) full-width at half-maximum. Note that, although the image preprocessing was performed in the resized scales, the results of VBM analysis were displayed in the original scales.

Histological analysis

We examined changes in neurogenesis, the number of astrocytes and neurite outgrowth in the ventral and dorsal hippocampi histologically. Fifteen weeks after the coronary ligation or the sham operation protocol, HF ($n = 8$) and sham rats ($n = 8$) were injected with bromodeoxyuridine (BrdU, 50 mg/kg i.p.) for 7 days to label dividing cells. One day after the final BrdU injection, the rats were transcardially perfused first with phosphate buffered saline (PBS, pH 7.4) and then with paraformaldehyde in PBS (4% PFA). The brains were carefully

removed from the skull, post-fixed in 4% PFA, and embedded in paraffin. Twenty consecutive 3- μ m coronal sections were obtained from the dorsal (approximately -2.8 to -3.8 from the bregma) and the ventral hippocampi (approximately -5.8 to -6.8 from the bregma). For measurement of neurogenesis, three randomly chosen sections in the dorsal and ventral hippocampi respectively were incubated with sheep anti-BrdU (1:50; abcam), a neurogenesis marker, and mouse anti-NeuN (neuronal nuclei, 1:500; Chemicom), a neuronal marker, for clarification of the dentate gyrus. Neurogenesis was measured by counting the number of BrdU-positive cells in the dorsal and ventral hippocampi. For analyses of astrocytes and neurite outgrowth, sections in the dorsal and ventral hippocampi were incubated with rabbit anti-GFAP (glial fibrillary acidic protein, 1:1000; Chemicom), an astrocyte marker, and mouse anti-MAP2 (microtubule-associated protein 2, 1:500; abcam), a neurite marker. Quantification of GFAP and MAP2 immunoreactivity was performed as modified in the past study (Ferreira et al., 2011; Calvo-Ochoa et al., 2014). Briefly, the number of GFAP positive cells was counted in four $\times 40$ magnification images of the hilus. Only astrocytes with complete processes and nuclei were selected. MAP2 densitometry was performed by automatically calculating the mean pixel intensity in four $\times 20$ magnification images of the hilus using ImageJ (<http://imagej.nih.gov/>). MAP2 density data were expressed as values relative to the average of sham rats. All the sections were finally incubated with the corresponding secondary antibodies and were examined using a fluorescence microscope (BZ-9000, Keyence, Osaka, Japan). Cardiac variables evaluated with echocardiography were not significantly different between the rats undergoing MRI recordings followed by behavioral tests and the rats undergoing histological analysis (Supplementary table).

Statistical analysis

To reveal regional changes in gray matter due to HF, the GMC maps of HF rats were compared to those obtained from sham rats using a Student's t-test at each voxel. We excluded all voxels with a gray matter probability value below 0.2 to include only voxels with sufficient gray matter proportion and avoid possible edge effects between gray matter and white matter or cerebrospinal fluid (May et al., 2007). The significance level was first set at $P < 0.05$ corrected for multiple comparisons using the false-discovery rate method (FDR corrected) with a minimum cluster size of 200 voxels (Suzuki et al., 2013b). Second, more stringent threshold of $P < 0.05$ corrected for multiple comparisons using the family-wise error method (FWE corrected) was applied to the comparison of the GMC maps. Consequently, the clusters in the bilateral hippocampus (Figs. 2C, D), whose focuses only survived with a threshold of $P < 0.05$ FWE corrected, were considered as a region of interest (ROI) and subjected to the following correlation analyses (Zhang et al., 2011; Suzuki et al., 2013b).

To investigate whether the 24 hour locomotor activity is associated with the GMC change, correlation analyses using the Pearson correlation coefficient were applied to 24 hour locomotor activity and mean

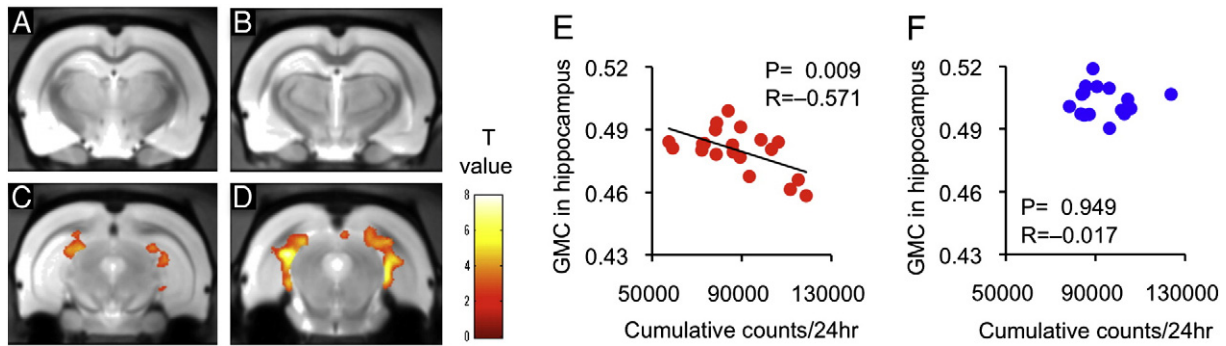


Fig. 2. VBM results comparing HF rats to sham rats (A–D) and the correlation between 24 hour locomotor activity and GMC values in the ventral hippocampus in HF (E) and sham rats (F). The results were displayed on the custom template that included both groups at -2.8 mm (A), -3.8 mm (B), -5.8 mm (C) and -6.8 mm (D) from the bregma. (A, B) and (C, D) correspond to the dorsal and ventral hippocampus respectively. The color calibration bars represent the critical T-score magnitudes with a threshold level of $P < 0.05$ FDR corrected. The center of the GMC decrease was exceeded at $P < 0.05$ FWE corrected, FDR corrected, corrected for multiple comparisons using the false discovery rate method; FWE corrected, corrected for multiple comparisons using the family wise error method; GMC, gray matter concentration; HF, heart failure; VBM, voxel based morphometry.

gray matter probability values inside the ROI at a significance level of $P < 0.05$. Because HF rats exhibited significant changes in cardiac variables and GMC compared to sham rats, all the correlation and regression analyses were performed in each of HF or sham rats to avoid biasing the association. We next applied univariate and multivariate regression analyses to 24 hour locomotor activity, the mean gray matter probability values inside the ROI, and cardiac variables including HW/BW ratio, infarct size, FS, LVDd, and PWTd. For multivariate analysis, stepwise backward elimination was selected to identify independent variables associated with 24 hour locomotor activity. The significance level of the regression analyses was set at $P < 0.05$.

We finally performed voxel-based correlation analysis based on the general linear model in the SPM8 toolbox to confirm the association between 24 hour locomotor activity and GMC values in the ventral hippocampus, which was supported by the regression analyses. For the voxel-based correlation analysis, we included only significant voxels that were identified by the comparison between the sham and HF rats using the significant voxel map ($P < 0.05$, FDR corrected with a minimum cluster size of 200 voxels) as the “inclusive mask” (i.e., small volume correction) as described in our previous studies (Takeuchi et al., 2010; Sumiyoshi et al., 2014). In the voxel-based correlation analysis, an uncorrected P value of < 0.001 was considered significant for the ventral hippocampus based on a priori hypothesis of the association between 24 hour locomotor activity and GMC values in the ventral hippocampus, which was identified by the regression analyses. We also analyzed the correlation between 24 hour locomotor activity and GMC values inside the ROI, which corresponded to significant clusters in the voxel-based correlation analysis, at a significance level of $P < 0.05$.

The body weight (BW), heart weight (HW)/BW ratio, infarct size, FS, LVDd, PWTd, 24 hour locomotor activity, the number of BrdU-positive cells, the number of GFAP-positive cells and relative MAP2 density are expressed as the mean \pm standard error of mean (SEM) and were analyzed using Student's t-tests at a significance level of $P < 0.05$. All statistical tests were two-tailed.

Results

Validation of a rat model of HF

Sixteen weeks after the coronary ligation, HF rats had significantly increased heart weight and infarcted regions compared with sham rats (Table 1). Moreover, significant decrease in FS and increase in LVDd and PWTd were observed with echocardiography in HF rats as compared with sham rats (Fig. 1, Table 1). These findings were consistent with cardiac remodeling in patients with ischemic HF (Sutton and Sharpe, 2000) and provides support for using the model described here as a valid model of patients with HF.

Structural abnormality of the ventral hippocampus in HF rats

To support our first hypothesis, the ventral hippocampus showed significant changes in VBM and histological analysis in HF rats as compared with sham rats. VBM successfully revealed significant GMC decrease in the hippocampus, medial septal nucleus, pons, amygdala, somatosensory cortex, cerebellum, motor cortex, striatum, subiculum, hypothalamus, periaqueductal gray and olfactory bulb in HF rats as compared with sham rats ($P < 0.05$ FDR corrected, Table 2, Supplementary figure). The cluster in the bilateral hippocampus, whose centers achieve a significance of $P < 0.05$ FWE corrected (Table 2), did not extend to the dorsal hippocampus (Figs. 2A, B) and were restricted to the ventral segment (Figs. 2C, D). Similarly, the number of BrdU-positive cells, the number of GFAP-positive cells and relative MAP2 density were not different between the two groups in the dorsal hippocampus (Figs. 3A, C, E) but the number of BrdU-positive cells and relative MAP2 density were significantly decreased and the number of GFAP-positive cells was significantly increased in HF rats as compared with sham rats in the ventral hippocampus (Figs. 3B, D, F), supporting our second hypothesis. These results indicated that the ventral hippocampus is more vulnerable in HF as is similar with depression (Willard et al., 2009; Tanti and Belzung, 2013).

Association between structural abnormality of the ventral hippocampus and depressive symptoms in HF rats

Contrary to our third hypothesis, 24 hour locomotor activity was not significantly different between HF rats and sham rats (Table 1). Results of 24 hour locomotor activity might be confounded by exercise intolerance in HF rats compared to sham rats. To investigate our fourth hypothesis, we first performed correlation analyses between GMC

Table 1

Cardiac variables and 24 hour locomotor activity in HF rats compared to sham rats undergoing MRI recording.

	Sham (N = 17)	HF (N = 20)	P value
BW (g)	555.9 \pm 27.1	549.3 \pm 38.9	0.557
HW/BW	2.5 \pm 0.2	3.4 \pm 0.6	0.000
Infarct size (%)	0	37.2 \pm 6.1	0.000
FS (%)	48.4 \pm 6.4	14.1 \pm 4.9	0.000
LVDd (mm)	8.3 \pm 0.4	12.0 \pm 0.9	0.000
PWTd (mm)	1.6 \pm 0.1	1.9 \pm 0.3	0.000
24 h locomotor (Counts/24 h)	93,744 \pm 2746	87,642 \pm 3879	0.222

BW, body weight; FS, fractional shortening; HF, heart failure; HW, heart weight; LVDd, left ventricular diastolic diameter; PWTd, posterior wall thickness in diastole; 24 h locomotor, 24 hour locomotor activity.

Table 2
Decreases in gray matter concentration in HF rats compared to sham rats.

	Coordinates (x, y, z)	Z score	Voxels in cluster
Hippocampus	(−3.6, −4.34, −6.72)	5.98	3886 (41)*
	(3.72, −5.78, −6.96)	5.32	4504 (1)*
	(0.48, −4.46, −0.36)	5.18	1092
	(3.72, −5.78, −6.98)	4.9	895
	(−0.12, −4.34, −2.88)	4.77	1018
	(−5.4, −4.22, −4.32)	4.46	200
Pons	(4.68, −3.02, −3.6)	4.26	246
	(1.32, −7.1, −9.96)	4.71	1023
Medial septal nucleus	(−0.48, −7.1, −12)	4.18	302
	(−0.12, −6.86, 0.12)	4.48	1645
Amygdala	(−3.36, −7.94, −5.52)	4.44	556
Somatosensory cortex	(4.44, −9.5, −3.72)	3.96	321
	(5.16, −2.66, 3)	4.23	414
Cerebellum	(−0.24, −1.58, −10.44)	4.05	294
	(4.2, −7.34, −11.76)	4.03	1340
Motor cortex	(2.28, −1.34, 2.88)	4.03	735
	(−0.96, −0.86, 2.76)	3.66	510
	(3.24, −3.02, 5.04)	3.63	322
Striatum	(−3.84, −7.7, −0.48)	3.92	271
Subiculum	(−6, −6.26, −7.32)	3.71	252
Hypothalamus	(1.44, −9.5, −3.84)	3.7	223
Periaqueductal gray	(−0.48, −5.42, −5.16)	3.67	221
Olfactory bulb	(0.48, −6.62, 5.16)	3.5	237

Coordinates are relative to bregma in the medial-lateral (x), superior-inferior (y), and anterior-posterior (z) directions (mm). Voxels in cluster are expressed as the number of voxels exceeding the threshold of $P < 0.05$ corrected for multiple comparisons using the false-discovery error method. *The center of the GMC decrease was exceeded at $P < 0.05$ corrected for multiple comparisons using the family-wise error method (FWE corrected). The numbers inside parentheses are significant voxels exceeding the threshold of $P < 0.05$ FWE corrected. HF, heart failure.

values in the ventral hippocampus and 24 hour locomotor activity in each of HF or sham rats. To support our fourth hypothesis, GMC values in the ventral hippocampus were significantly and negatively correlated with 24 hour locomotor activity in HF rats (Fig. 2E) but not in sham rats (Fig. 2F). We next performed univariate and multivariate regression analyses among 24 hour locomotor activity, GMC values in the ventral hippocampus and cardiac variables in each of HF or sham rats. Univariate regression analysis showed that 24 hour locomotor activity was significantly associated with GMC values in the ventral hippocampus and infarct size in HF rats (Table 3). Multivariate regression analysis demonstrated that the best model predicting 24 hour locomotor activity consisted of GMC values in the ventral hippocampus, infarct size and fractional shortening in HF rats (Table 4). Either univariate or multivariate regression analyses did not show any significant association in sham rats. Therefore, GMC values in the ventral hippocampus remained to be significantly associated with 24 hour locomotor activity even after adjustment of infarct size and FS. Moreover, the significant correlation between 24 hour locomotor activity and GMC values in the ventral hippocampus was also observed in a voxel-based correlation analysis in HF rats (Fig. 4, Table 5). In contrast, no voxels survived at a significance level of $P < 0.001$ uncorrected for multiple comparisons in a voxel-based correlation analysis in sham rats. These results support the view that the structural abnormality of the ventral hippocampus is associated with depressive symptoms in HF.

Discussions

The major findings of the present study were as follows: (1) Structural abnormalities in the ventral hippocampus such as decrease in GMC, neurogenesis and neurite outgrowth and increase in the number of astrocytes occur as a result of HF in rats. (2) There was a significant negative correlation between GMC in the ventral hippocampus and 24 hour locomotor activity in HF rats. To the best of our knowledge, the present study provides the first evidence to suggest that the structural abnormalities in the ventral hippocampus are associated with depressive symptoms in HF.

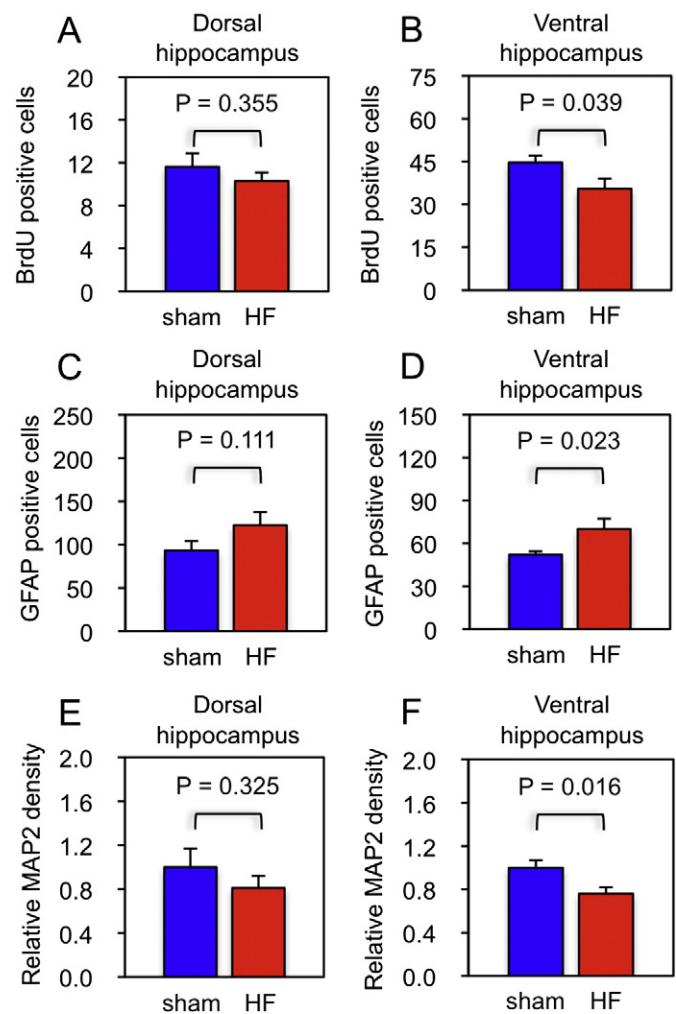


Fig. 3. Results of histological analysis comparing HF rats to sham rats. Quantification of the number of BrdU-positive cells (A, B), the number of GFAP positive cells (C, D) and relative MAP2 density (E, F) in the dorsal (A, C, E) or ventral hippocampus (B, D, F) in HF rats and sham rats. MAP2 density data relative to sham rats were shown in HF rats. BrdU, bromodeoxyuridine; GFAP, glial fibrillary acidic protein; HF, heart failure; MAP2, microtubule-associated protein 2.

Brain structural abnormality in HF rats

In the present study, the ventral hippocampus, which relates to the processing of emotion (Kjelstrup et al., 2002; Fanselow and Dong, 2010), showed a significant decrease in GMC, neurogenesis and neurite outgrowth and increase in the number of astrocytes in HF rats as compared with sham rats. The structural abnormality of the ventral hippocampus in HF was consistent with that found in behaviorally depressed cynomolgus macaques and rodents (Willard et al., 2009; Tanti and Belzung, 2013) and thus had been hypothesized before the experiment due to the high prevalence of depression in HF patients (Rutledge et al., 2006). The coexistence of a decrease in GMC and histological changes in the ventral hippocampus supported the view that MRI-detectable alterations in gray matter reflect histological changes (Zatorre et al., 2012; Lerch et al., 2011; Suzuki et al., 2013b). Although adult neurogenesis-derived neurons are a relatively small portion of the total number of hippocampal neurons (Zatorre et al., 2012), adult neurogenesis has been reported to buffer depressive symptoms (Snyder et al., 2011). Therefore, decreased neurogenesis might be indirectly associated with GMC decreases in the ventral hippocampus in HF through an exacerbation of depressive symptoms. The increase in the number of astrocytes was not consistent with reduction in the number

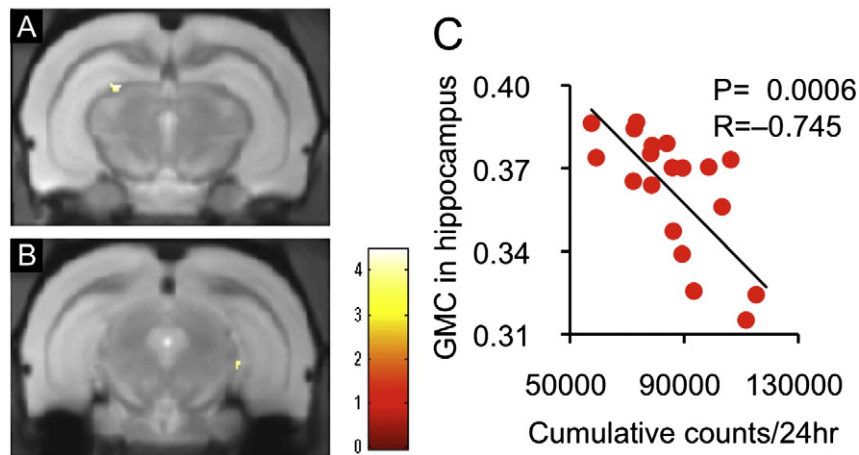


Fig. 4. Results of voxel-based correlation analysis for 24-hour locomotor activity in HF rats. The results (A, B) were displayed on the custom template that included 20 HF rats. The color calibration bars represent the critical T-score magnitudes with a threshold level of $P < 0.001$ uncorrected for multiple comparisons. The graph (C) showed the correlation between 24-hour locomotor activity and GMC values inside the ROI, which corresponded to significant clusters in the voxel-based correlation analysis. GMC, gray matter concentration; HF, heart failure.

of astrocytes in postmortem brains of depressed patients (Harrison, 2002). The discrepancy between the result of this study and human findings can be explained by the idea that stress activates astrocytes and induces to increase the number of astrocytes in acute resistance stage, and finally chronic stress tires astrocytes and the number of astrocytes is decreased in chronic exhaustion stage (Iwata et al., 2011; Sugama et al., 2011). Proliferation of astrocytes in the brain region with reduction in gray matter did not support the view that the explanation for MRI volume increases is an increase in the number of non-neuronal cells (Zatorre et al., 2012) but was consistent with our previous study that GMC values were negatively correlated with the number of microglia (Suzuki et al., 2013b). The contribution of glia to MRI-detectable gray matter changes should be reevaluated in the future studies. The GMC decrease concomitant with reduction in neurite outgrowth, which was also observed in animal models of depression (Watanabe et al., 1992; Reinés et al., 2008), was consistent with the past study that axonal remodeling was correlated with MRI-detectable volume changes in learning exercise (Lerch et al., 2011). Therefore, neurite outgrowth might reflect HF-induced GMC changes in the ventral hippocampus.

VBM also revealed that GMC decreases in the dorsal hippocampus, medial septal nucleus, pons, amygdala, subiculum, hypothalamus, periaqueductal gray and olfactory bulb in HF rats as compared with sham rats at a significance threshold of $P < 0.05$, FDR corrected. The dorsal (posterior in humans) hippocampus primarily performs memory function (Broadbent et al., 2004; Fanselow and Dong, 2010). Gray matter decreases in the posterior hippocampus are observed and associated with reduced memory performance in mild cognitive impairment, the precursor to Alzheimer's disease (Schmidt-Wilcke et al., 2009). Memory impairment is also reported in patients with HF (Vogels et al., 2007). Therefore, it might be reasonable to expect GMC decreases in the dorsal

hippocampus in HF rats even though histological changes were not observed in HF rats as compared with sham rats.

HF is characterized by overactivity of sympathetic nervous system, in which low cardiac output causes reduction in effective circulating plasma volume (Triposkiadis et al., 2009). Changes in the number of glial cells in the hypothalamus mediates sympathetic overactivity in HF (Yu et al., 2010) and may also cause exaggerated hypothalamus–pituitary adrenal axis (Gerber and Bale, 2012), which can damage brain regions with high density of glucocorticoid receptors such as the hippocampus and amygdala (Sapolsky, 2000; Johnson et al., 2005). Periaqueductal gray and pons, which are downstream targets of the hypothalamus, modulate cardiac sympathetic functions in rats (Farkas et al., 1998) and may be associated with aberrant sympathetic arousal in HF in combination with the hypothalamus (Triposkiadis et al., 2009). The number of astrocytes in amygdala, periaqueductal gray or pontine locus coeruleus is changed in acute or chronic stress or major depression (Sugama et al., 2011; Imbe et al., 2012; Chandley et al., 2013). A meta analysis of MRI studies revealed decrease in amygdala volume in unmedicated depressed individuals (Hamilton et al., 2008). These evidences may indicate that the GMC decreases in the hippocampus, amygdala, hypothalamus, periaqueductal gray and pons are associated with the enhancement of sympathetic nervous system and/or hypothalamus–pituitary adrenal axis in HF. The medial septal nucleus, subiculum and olfactory bulb have neuronal connections with the ventral hippocampus (Fanselow and Dong, 2010), which could explain the reductions in GMC in these brain regions.

Possible mechanisms of brain structural abnormality in HF rats

Potential mechanisms of brain structural abnormalities in HF rats include the possibility that low cardiac output in HF induces cerebral hypoxia. The association between cardiac index and total brain volume has been reported from the Framingham Offspring Cohort (Jefferson et al., 2010). In contrast, however, we previously demonstrated that CA1 region of the dorsal hippocampus was mainly affected in a rat model of cardiac arrest and resuscitation (Suzuki et al., 2013b), which

Table 3
Univariate regression analysis for 24-hour locomotor activity in HF rats.

	Estimate	P value
GMC in hippocampus	−958,147	0.009
HW/BW	884	0.900
Infarct size (%)	1319	0.040
FS (%)	426	0.614
LVDd (mm)	−1506	0.753
PWTd (mm)	9637	0.499

BW, body weight; FS, fractional shortening; GMC, gray matter concentration; HF, heart failure; HW, heart weight; LVDd, left ventricular diastolic diameter; PWTd, posterior wall thickness in diastole.

Table 4
Multivariate regression analysis for 24-hour locomotor activity in HF rats.

	Estimate	P value
GMC in hippocampus	−843,777	0.011
Infarct size (%)	1377	0.020
FS (%)	1417	0.043

FS, fractional shortening; GMC, gray matter concentration; HF, heart failure.

Table 5

Brain regions containing significant correlation voxels between 24 hour locomotor activity and regional gray matter concentration in HF rats.

	Coordinates (x, y, z)	Z score	Voxels in cluster
Hippocampus	(−2.28, −3.86, −4.92)	3.62	41
	(3.6, −6.26, −5.76)	3.34	14

Coordinates are relative to bregma in the medial-lateral (x), superior-inferior (y), and anterior-posterior (z) directions (mm). Voxels in cluster are expressed as the number of voxels exceeding the threshold of $P < 0.001$ uncorrected for multiple comparisons. HF, heart failure.

is not consistent with GMC decrease primarily in the ventral hippocampus in HF rats. Moreover, both acute and chronic cerebral hypoperfusion increase hippocampal neurogenesis (Kokaia and Lindvall, 2003; Sivilia et al., 2008) in spite of gliosis and MAP-2 loss in CA1 region of the dorsal hippocampus (De la Torre, 2000). Therefore, the impact of cardiac output on brain structural abnormality in HF is controversial at this moment. Second, stress and resultant increase in blood glucocorticoid level in HF (Bremner, 1999; Güder et al., 2007) decreases gray matter in the hippocampus and inhibits neurogenesis (Mirescu and Gould, 2006). Changes in the number of astrocytes and neurite outgrowth are also induced by stress (Watanabe et al., 1992; Reinés et al., 2008; Iwata et al., 2011; Sugama et al., 2011). This system can form a positive feedback loop because decreased neurogenesis leads to an increased glucocorticoid response to stress (Snyder et al., 2011). These possible mechanisms should be investigated in the future studies.

Implications of the present study

The present study demonstrated an association between structural abnormality of the ventral hippocampus and depression in HF. The present study implicates a novel neural substrate to explain the vicious circle between HF and depression. The prevalence of depression is increased in HF patients (Rutledge et al., 2006), whereas depression complicated with HF is associated with increased risk of mortality and rehospitalization in patients with HF (Jiang et al., 2001; Rutledge et al., 2006). Antidepressants and exercise training improve symptoms in patients with depression (Ströhle, 2009; Fournier et al., 2010), increase gray matter, neurogenesis and neurite outgrowth in the hippocampus (Malberg et al., 2000; Redila and Christie, 2006; van Praag et al., 2005; Reinés et al., 2008; Erickson et al., 2011; Arnone et al., 2013) and recover the proliferation of astrocytes induced by depression (Iwata et al., 2011; Eyre et al., 2013).

In patients with heart failure, exercise training reduces depressive symptoms and composite of death or hospitalization (Blumenthal et al., 2012) but antidepressants have not provided an effect of reducing depressive symptoms or treating depression on clinical outcomes (O'Connor et al., 2010). The positive effects of exercise in patients with heart failure may be mediated by improving structural abnormalities in the ventral hippocampus.

Limitations of the present study

Limitations of the present study include the fact that 24 hour locomotor activity was not significantly different between the two groups. Exercise intolerance and increased thirst in HF rats (Pfeifer et al., 2001; De Smet et al., 2003) can also affect results of other behavioral studies for assessment of depression-like behavior such as the forced swim test, tail suspension test or sucrose preference test (Ge et al., 2013). Therefore, it is possible that exercise intolerance in HF rats (Pfeifer et al., 2001) confounded 24 hour locomotor activity. Despite the difficulties involved in assessing depressive symptoms, the present study clearly showed the association between decreased GMC values in the ventral hippocampus and increased 24 hour locomotor activity in HF rats. Second, neuroanatomical differences are not negligible between rats and humans (Craig, 2009) in spite of the conservation of

hippocampal function and structure between the two species (Squire, 1992). Although there are many confounding factors (Ward et al., 2010; Zhang et al., 2011; Glodzik et al., 2012; Moran et al., 2013), the findings in the present study should be reevaluated in patients with HF. On the other hand, an animal MRI study has several advantages compared to a human study such as availability of histological analysis (Lerch et al., 2011; Zatorre et al., 2012; Suzuki et al., 2013b) and molecular intervention (Ellegood et al., 2012; Steadman et al., 2014), and thus can be useful for evaluating the mechanism of alteration in brain structures in humans.

Conclusions

The present study demonstrated for the first time that the structural abnormalities of the ventral hippocampus are associated with depressive symptoms in HF rats.

Acknowledgments

The authors would like to thank Ms. Yumi Watanabe and Mr. Hiroi Nonaka for her assistance with histological preparations and analyses and his technical assistance. In addition, we would like to thank Tohoku University International Advanced Research and Education Organization for supporting our research.

Conflict of interest

There is no conflict of interest in this study.

Appendix A. Supplementary data

Supplementary data to this article can be found online at <http://dx.doi.org/10.1016/j.neuroimage.2014.10.040>.

References

- Almeida, O.P., Garrido, G.J., Beer, C., Lautenschlager, N.T., Arnolda, L., Flicker, L., 2012. Cognitive and brain changes associated with ischaemic heart disease and heart failure. *Eur. Heart J.* 33, 1769–1776.
- Arnone, D., McKie, S., Elliott, R., Juhasz, G., Thomas, E.J., Downey, D., Williams, S., Deakin, J.F., Anderson, I.M., 2013. State-dependent changes in hippocampal grey matter in depression. *Mol. Psychiatry* 18, 1265–1272.
- Ashburner, J., 2007. A fast diffeomorphic image registration algorithm. *NeuroImage* 38, 95–113.
- Ashburner, J., Friston, K.J., 2000. Voxel-based morphometry—the methods. *NeuroImage* 11, 805–821.
- Ashburner, J., Friston, K.J., 2001. Why voxel-based morphometry should be used. *NeuroImage* 14, 1238–1243.
- Ashburner, J., Friston, K.J., 2005. Unified segmentation. *NeuroImage* 26, 839–851.
- Biedermann, S., Fuss, J., Zheng, L., Sartorius, A., Falfán-Melgoza, C., Demirakca, T., Gass, P., Ende, G., Weber-Fahr, W., 2012. In vivo voxel based morphometry: detection of increased hippocampal volume and decreased glutamate levels in exercising mice. *NeuroImage* 61, 1206–1212.
- Blumenthal, J.A., Babyak, M.A., O'Connor, C., Keteyian, S., Landzberg, J., Howlett, J., Kraus, W., Gottlieb, S., Blackburn, G., Swank, A., Whellan, D.J., 2012. Effects of exercise training on depressive symptoms in patients with chronic heart failure: the HF-ACTION randomized trial. *JAMA* 308, 465–474.
- Bremner, J.D., 1999. Does stress damage the brain? *Biol. Psychiatry* 45, 797–805.
- Broadbent, N.J., Squire, L.R., Clark, R.E., 2004. Spatial memory, recognition memory, and the hippocampus. *Proc. Natl. Acad. Sci. U. S. A.* 101, 14515–14520.
- Calvo-Ochoa, E., Hernandez-Ortega, K., Ferrera, P., Morimoto, S., Arias, C., 2014. Short-term high-fat-and-fructose feeding produces insulin signaling alterations accompanied by neurite and synaptic reduction and astroglial activation in the rat hippocampus. *J. Cereb. Blood Flow Metab.* 34, 1001–1008.
- Chandley, M.J., Szebeni, K., Szebeni, A., Crawford, J., Stockmeier, C.A., Turecki, G., Miguel-Hidalgo, J.J., Ordway, G.A., 2013. Gene expression deficits in pontine locus coeruleus astrocytes in men with major depressive disorder. *J. Psychiatry Neurosci.* 38, 276–284.
- Craig, A.D., 2009. A rat is not a monkey is not a human: comment on Mogil (Nature Rev. Neurosci. 10, 283–294 (2009)). *Nat. Rev. Neurosci.* 10, 466.
- De la Torre, J.C., 2000. Critically attained threshold of cerebral hypoperfusion: the CATCH hypothesis of Alzheimer's pathogenesis. *Neurobiol. Aging* 21, 331–342.
- De Smet, H.R., Menadue, M.F., Oliver, J.R., Phillips, P.A., 2003. Increased thirst and vasopressin secretion after myocardial infarction in rats. *Am. J. Physiol. Regul. Integr. Comp. Physiol.* 285, R1203–R1211.

- Ellegood, J., Henkelman, R.M., Lerch, J.P., 2012. Neuroanatomical assessment of the integrin $\beta 3$ mouse model related to autism and the serotonin system using high resolution MRI. *Front. Psychiatry* 3, 37.
- Erickson, K.I., Voss, M.W., Prakash, R.S., Basak, C., Szabo, A., Chaddock, L., Kim, J.S., Heo, S., Alves, H., White, S.M., Wojcicki, T.R., Mailey, E., Vieira, V.J., Martin, S.A., Pence, B.D., Woods, J.A., McAuley, E., Kramer, A.F., 2011. Exercise training increases size of hippocampus and improves memory. *Proc. Natl. Acad. Sci. U. S. A.* 108, 3017–3022.
- Eyre, H.A., Papps, E., Baune, B.T., 2013. Treating depression and depression-like behavior with physical activity: an immune perspective. *Front. Psychiatry* 4, 3.
- Fanselow, M.S., Dong, H.W., 2010. Are the dorsal and ventral hippocampus functionally distinct structures? *Neuron* 65, 7–19.
- Farkas, E., Jansen, A.S., Loewy, A.D., 1998. Periaqueductal gray matter input to cardiac-related sympathetic premotor neurons. *Brain Res.* 792, 179–192.
- Ferreira, A.F., Real, C.C., Rodrigues, A.C., Alves, A.S., Britto, L.R., 2011. Short-term, moderate exercise is capable of inducing structural, BDNF-independent hippocampal plasticity. *Brain Res.* 1425, 111–122.
- Fournier, J.C., DeRubeis, R.J., Hollon, S.D., Dimidjian, S., Amsterdam, J.D., Shelton, R.C., Fawcett, J., 2010. Antidepressant drug effects and depression severity: a patient-level meta-analysis. *JAMA* 303, 47–53.
- Fukumauchi, F., Mataga, N., Wang, Y.J., Sato, S., Youshiki, A., Kusakabe, M., 1996. Abnormal behavior and neurotransmissions of tenascin gene knockout mouse. *Biochem. Biophys. Res. Commun.* 221, 151–156.
- Ge, J.F., Qi, C.C., Zhou, J.N., 2013. Imbalance of leptin pathway and hypothalamus synaptic plasticity markers are associated with stress-induced depression in rats. *Behav. Brain Res.* 249, 38–43.
- Gerber, A.R., Bale, T.L., 2012. Antiinflammatory treatment ameliorates HPA stress axis dysfunction in a mouse model of stress sensitivity. *Endocrinology* 153, 4830–4837.
- Glodzik, L., Mosconi, L., Tsui, W., de Santi, S., Zinkowski, R., Pirraglia, E., Rich, K.E., McHugh, P., Li, Y., Williams, S., Ali, F., Zetterberg, H., Blennow, K., Mehta, P., de Leon, M.J., 2012. Alzheimer's disease markers, hypertension, and gray matter damage in normal elderly. *Neurobiol. Aging* 33, 1215–1227.
- Güder, G., Bauersachs, J., Frantz, S., Weismann, D., Alolio, B., Ertl, G., Angermann, C.E., Störk, S., 2007. Complementary and incremental mortality risk prediction by cortisol and aldosterone in chronic heart failure. *Circulation* 115, 1754–1761.
- Hamilton, J.P., Siemer, M., Gotlib, I.H., 2008. Amygdala volume in major depressive disorder: a meta-analysis of magnetic resonance imaging studies. *Mol. Psychiatry* 13, 993–1000.
- Harrison, P.J., 2002. The neuropathology of primary mood disorder. *Brain* 125, 1428–1449.
- Henderson, K.K., Danzi, S., Paul, J.T., Leya, G., Klein, I., Samarel, A.M., 2009. Physiological replacement of T3 improves left ventricular function in an animal model of myocardial infarction-induced congestive heart failure. *Circ. Heart Fail.* 2, 243–252.
- Imbe, H., Kimura, A., Donishi, T., Kaneoke, Y., 2012. Chronic restraint stress decreases glial fibrillary acidic protein and glutamate transporter in the periaqueductal gray matter. *Neuroscience* 223, 209–218.
- Iwata, M., Shirayama, Y., Ishida, H., Hazama, G.I., Nakagome, K., 2011. Hippocampal astrocytes are necessary for antidepressant treatment of learned helplessness rats. *Hippocampus* 21, 877–884.
- Jefferson, A.L., Himali, J.J., Beiser, A.S., Au, R., Massaro, J.M., Seshadri, S., Gona, P., Salton, C.J., DeCarli, C., O'Donnell, C.J., Benjamin, E.J., Wolf, P.A., Manning, W.J., 2010. Cardiac index is associated with brain aging: the Framingham Heart Study. *Circulation* 122, 690–697.
- Jiang, W., Alexander, J., Christopher, E., Kuchibhatla, M., Gaudin, L.H., Cuffe, M.S., Blazing, M.A., Davenport, C., Califf, R.M., Krishnan, R.R., O'Connor, C.M., 2001. Relationship of depression to increased risk of mortality and rehospitalization in patients with congestive heart failure. *Arch. Intern. Med.* 161, 1849–1856.
- Johnson, L.R., Farb, C., Morrison, J.H., McEwen, B.S., LeDoux, J.E., 2005. Localization of glucocorticoid receptors at postsynaptic membranes in the lateral amygdala. *Neuroscience* 136, 289–299.
- Kabuki, Y., Mizobe, Y., Yamada, S., Furuse, M., 2009. Dietary L-tyrosine alleviates the behavioral alterations induced by social isolation stress in mice. *Brain Res. Bull.* 80, 389–396.
- Kjelstrup, K.G., Tuvnes, F.A., Steffenach, H.A., Murison, R., Moser, E.I., Moser, M.B., 2002. Reduced fear expression after lesions of the ventral hippocampus. *Proc. Natl. Acad. Sci. U. S. A.* 99, 10825–10830.
- Klein, A., Andersson, J., Ardekani, B.A., Ashburner, J., Avants, B., Chiang, M.C., Christensen, G.E., Collins, D.L., Gee, J., Hellier, P., Song, J.H., Jenkinson, M., Lepage, C., Rueckert, D., Thompson, P., Vercauteren, T., Woods, R.P., Mann, J.J., Parsey, R.V., 2009. Evaluation of 14 nonlinear deformation algorithms applied to human brain MRI registration. *NeuroImage* 46, 786–802.
- Kokaia, Z., Lindvall, O., 2003. Neurogenesis after ischaemic brain insults. *Curr. Opin. Neurobiol.* 13, 127–132.
- Lerch, J.P., Yiu, A.P., Martinez-Canabal, A., Pekar, T., Bohbot, V.D., Frankland, P.W., Henkelman, R.M., Josselyn, S.A., Sled, J.G., 2011. Maze training in mice induces MRI-detectable brain shape changes specific to the type of learning. *NeuroImage* 54, 2086–2095.
- Malberg, J.E., Eisch, A.J., Nestler, E.J., Duman, R.S., 2000. Chronic antidepressant treatment increases neurogenesis in adult rat hippocampus. *J. Neurosci.* 20, 9104–9110.
- May, A., Hajak, G., Gänssbauer, S., Steffens, T., Langguth, B., Kleinjung, T., Eichhammer, P., 2007. Structural brain alterations following 5 days of intervention: dynamic aspects of neuroplasticity. *Cereb. Cortex* 17, 205–210.
- Menteer, J., Macey, P.M., Woo, M.A., Panigrahy, A., Harper, R.M., 2010. Central nervous system changes in pediatric heart failure: a volumetric study. *Pediatr. Cardiol.* 31, 969–976.
- Mirescu, C., Gould, E., 2006. Stress and adult neurogenesis. *Hippocampus* 16, 233–238.
- Moran, C., Phan, T.G., Chen, J., Blizard, L., Beare, R., Venn, A., Münch, G., Wood, A.G., Forbes, J., Greenaway, T.M., Pearson, S., Srikanth, V., 2013. Brain atrophy in type 2 diabetes: regional distribution and influence on cognition. *Diabetes Care* 36, 4036–4042.
- Morgan, E.E., Faulx, M.D., McElfresh, T.A., Kung, T.A., Zawaneh, M.S., Stanley, W.C., Chandler, M.P., Hoit, B.D., 2004. Validation of echocardiographic methods for assessing left ventricular dysfunction in rats with myocardial infarction. *Am. J. Physiol. Heart Circ. Physiol.* 287, H2049–H2053.
- O'Connor, C.M., Jiang, W., Kuchibhatla, M., Silva, S.G., Cuffe, M.S., Callwood, D.D., Zakhary, B., Stough, W.G., Arias, R.M., Rivelli, S.K., Krishnan, R., Investigators, S.A.D.H.A.R.T.-CHF, 2010. Safety and efficacy of sertraline for depression in patients with heart failure: results of the SADHART-CHF (Sertraline Against Depression and Heart Disease in Chronic Heart Failure) trial. *J. Am. Coll. Cardiol.* 56, 692–699.
- Okuda, T., Ito, Y., Nakagawa, N., Hishinuma, T., Tsukamoto, H., Iwabuchi, K., Watanabe, T., Kitaichi, K., Goto, J., Yanai, K., 2004. Drug interaction between methamphetamine and antihistamines: behavioral changes and tissue concentrations of methamphetamine in rats. *Eur. J. Pharmacol.* 505, 135–144.
- Pfeifer, P.C., Musch, T.I., McAllister, R.M., 2001. Skeletal muscle oxidative capacity and exercise tolerance in rats with heart failure. *Med. Sci. Sports Exerc.* 33, 542–548.
- Quallo, M.M., Price, C.J., Ueno, K., Asamizuya, T., Cheng, K., Lemon, R.N., Iriki, A., 2009. Gray and white matter changes associated with tool-use learning in macaque monkeys. *Proc. Natl. Acad. Sci. U. S. A.* 106, 18379–18384.
- Redila, V.A., Christie, B.R., 2006. Exercise-induced changes in dendritic structure and complexity in the adult hippocampal dentate gyrus. *Neuroscience* 137, 1299–1307.
- Reinés, A., Cereseto, M., Ferrero, A., Sifonios, L., Podestà, M.F., Wikinski, S., 2008. Maintenance treatment with fluoxetine is necessary to sustain normal levels of synaptic markers in an experimental model of depression: correlation with behavioral response. *Neuropsychopharmacology* 33, 1896–1908.
- Rutledge, T., Reis, V.A., Linke, S.E., Greenberg, B.H., Mills, P.J., 2006. Depression in heart failure: a meta-analytic review of prevalence, intervention effects, and associations with clinical outcomes. *J. Am. Coll. Cardiol.* 48, 1527–1537.
- Saeed, M., Lund, G., Wendland, M.F., Bremerich, J., Weinmann, H., Higgins, C.B., 2001. Magnetic resonance characterization of the peri-infarction zone of reperfused myocardial infarction with necrosis-specific and extracellular nonspecific contrast media. *Circulation* 103, 871–876.
- Sapolsky, R.M., 2000. Glucocorticoids and hippocampal atrophy in neuropsychiatric disorders. *Arch. Gen. Psychiatry* 57, 925–935.
- Sawiak, S.J., Wood, N.L., Williams, G.B., Morton, A.J., Carpenter, T.A., 2009. Voxel-based morphometry in the R6/2 transgenic mouse reveals differences between genotypes not seen with manual 2D morphometry. *Neurobiol. Dis.* 33, 20–27.
- Schmidt-Wilke, T., Poljansky, S., Hierlmeier, S., Hausner, J., Ibach, B., 2009. Memory performance correlates with gray matter density in the ento-/perirhinal cortex and posterior hippocampus in patients with mild cognitive impairment and healthy controls—a voxel based morphometry study. *NeuroImage* 47, 1914–1920.
- Sivilia, S., Giuliani, A., Del Vecchio, G., Giardino, L., Calzà, L., 2008. Age-dependent impairment of hippocampal neurogenesis in chronic cerebral hypoperfusion. *Neuropathol. Appl. Neurobiol.* 34, 52–61.
- Snyder, J.S., Soumier, A., Brewer, M., Pickel, J., Cameron, H.A., 2011. Adult hippocampal neurogenesis buffers stress responses and depressive behaviour. *Nature* 476, 458–461.
- Squire, L.R., 1992. Memory and the hippocampus: a synthesis from findings with rats, monkeys, and humans. *Psychol. Rev.* 99, 195–231.
- Steadman, P.E., Ellegood, J., Zulc, K.U., Turnbull, D.H., Joyner, A.L., Henkelman, R.M., Lerch, J.P., 2014. Genetic effects on cerebellar structure across mouse models of autism using a magnetic resonance imaging atlas. *Autism Res.* 7, 124–137.
- Ströhle, A., 2009. Physical activity, exercise, depression and anxiety disorders. *J. Neural Transm.* 116, 777–784.
- Sugama, S., Takenouchi, T., Sekiyama, K., Kitani, H., Hashimoto, M., 2011. Immunological responses of astroglia in the rat brain under acute stress: interleukin 1 beta colocalized in astroglia. *Neuroscience* 192, 429–437.
- Sumiyoshi, A., Suzuki, H., Ogawa, T., Riera, J.J., Shimokawa, H., Kawashima, R., 2012. Coupling between gamma oscillation and fMRI signal in the rat somatosensory cortex: its dependence on systemic physiological parameters. *NeuroImage* 60, 738–746.
- Sumiyoshi, A., Taki, Y., Nonaka, H., Takeuchi, H., Kawashima, R., 2014. Regional gray matter volume increases following 7 days of voluntary wheel running exercise: a longitudinal VBM study in rats. *NeuroImage* 98, 82–90.
- Sutton, M.G., Sharpe, N., 2000. Left ventricular remodeling after myocardial infarction: pathophysiology and therapy. *Circulation* 101, 2981–2988.
- Suzuki, H., Sumiyoshi, A., Kawashima, R., Shimokawa, H., 2013a. Different brain activation under left and right ventricular stimulation: an fMRI study in anesthetized rats. *PLoS ONE* 8, e56990.
- Suzuki, H., Sumiyoshi, A., Taki, Y., Matsumoto, Y., Fukumoto, Y., Kawashima, R., Shimokawa, H., 2013b. Voxel-based morphometry and histological analysis for evaluating hippocampal damage in a rat model of cardiopulmonary resuscitation. *NeuroImage* 77, 215–221.
- Takeuchi, H., Sekiguchi, A., Taki, Y., Yokoyama, S., Yomogida, Y., Komuro, N., Yamanouchi, T., Suzuki, S., Kawashima, R., 2010. Training of working memory impacts structural connectivity. *J. Neurosci.* 30, 3297–3303.
- Taki, Y., Hashizume, H., Thyreau, B., Sassa, Y., Takeuchi, H., Wu, K., Kotozaki, Y., Nouchi, R., Asano, M., Asano, K., Fukuda, H., Kawashima, R., 2012. Sleep duration during weekdays affects hippocampal gray matter volume in healthy children. *NeuroImage* 60, 471–475.
- Tanti, A., Belzung, C., 2013. Neurogenesis along the septo-temporal axis of the hippocampus: are depression and the action of antidepressants region-specific? *Neuroscience* 252, 234–252.
- Triposkiadis, F., Karayannis, G., Giamouzis, G., Skolarigis, J., Louridas, G., Butler, J., 2009. The sympathetic nervous system in heart failure physiology, pathophysiology, and clinical implications. *J. Am. Coll. Cardiol.* 54, 1747–1762.
- Valdés-Hernández, P.A., Nonaka, H., Haga, R., Vasquez, E.A., Ogawa, T., Medina, Y.I., Riera, J.J., Kawashima, R., 2011. An in vivo MRI template set for morphometry, tissue segmentation and fMRI localization in rats. *Front. Neuroinform.* 5, 26.

- van Praag, H., Shubert, T., Zhao, C., Gage, F.H., 2005. Exercise enhances learning and hippocampal neurogenesis in aged mice. *J. Neurosci.* 25, 8680–8685.
- Vogels, R.L., Scheltens, P., Schroeder-Tanka, J.M., Weinstein, H.C., 2007. Cognitive impairment in heart failure: a systematic review of the literature. *Eur. J. Heart Fail.* 9, 440–449.
- Ward, M.A., Bendlin, B.B., McLaren, D.G., Hess, T.M., Gallagher, C.L., Kastman, E.K., Rowley, H.A., Asthana, S., Carlsson, C.M., Sager, M.A., Johnson, S.C., 2010. Low HDL cholesterol is associated with lower gray matter volume in cognitively healthy adults. *Front. Aging Neurosci.* 2. <http://dx.doi.org/10.3389/fnagi.2010.00029> (pii: 29).
- Watanabe, Y., Gould, E., McEwen, B.S., 1992. Stress induces atrophy of apical dendrites of hippocampal CA3 pyramidal neurons. *Brain Res.* 588, 341–345.
- Willard, S.L., Friedman, D.P., Henkel, C.K., Shively, C.A., 2009. Anterior hippocampal volume is reduced in behaviorally depressed female cynomolgus macaques. *Psychoneuroendocrinology* 34, 1469–1475.
- Woo, M.A., Macey, P.M., Fonarow, G.C., Hamilton, M.A., Harper, R.M., 2003. Regional brain gray matter loss in heart failure. *J. Appl. Physiol.* 95, 677–684.
- Yang, J., Wadghiri, Y.Z., Hoang, D.M., Tsui, W., Sun, Y., Chung, E., Li, Y., Wang, A., de Leon, M., Wisniewski, T., 2011. Detection of amyloid plaques targeted by USPIO- $A\beta$ 1–42 in Alzheimer's disease transgenic mice using magnetic resonance microimaging. *NeuroImage* 55, 1600–1609.
- Yu, Y., Zhang, Z.H., Wei, S.G., Serrats, J., Weiss, R.M., Felder, R.B., 2010. Brain perivascular macrophages and the sympathetic response to inflammation in rats after myocardial infarction. *Hypertension* 55, 652–659.
- Zatorre, R.J., Fields, R.D., Johansen-Berg, H., 2012. Plasticity in gray and white: neuroimaging changes in brain structure during learning. *Nat. Neurosci.* 15, 528–536.
- Zhang, X., Salmeron, B.J., Ross, T.J., Geng, X., Yang, Y., Stein, E.A., 2011. Factors underlying prefrontal and insula structural alterations in smokers. *NeuroImage* 54, 42–48.